Grinding performance of electroplated diamond tools strengthened with Cr-C deposit using diamond particles in an average size of 150 μm

Ching An Huang
Chia Hsuan Shen (p.c.shen@outlook.com)
Chang Gung University
Wei Ze Huang
Jeng Shun Lo
Po Liang Lai

Research Article

Keywords: Cr-C deposit, electroplated diamond tool, hard-to-cut materials, slot grinding, fractographic study

Posted Date: March 25th, 2022

DOI: https://doi.org/10.21203/rs.3.rs-1458876/v1

Abstract

Electroplated diamond tools with single-layered high density diamond particles in an average size of 150 μm were prepared through a three-step electroplating process, including Ni-undercoating, Ni-diamond co-electrodeposition and Cr-C strengthening electroplating. Martensitic stainless steel (AISI 440C) rods with a diameter of 3 mm were used as substrates for tool fabrications. To evaluate tool grinding performances, linear slot grinding tests on the Al_2O_3 plates were conducted. The grinding performance of an electroplated diamond tool was determined through its maximum ground length upon tool failure. Experimental results show that an electroplated diamond tool with high density of diamond particles can be prepared by using Ni-diamond co-electrodeposition. After annealing at 500°C for 30 min, the hardness of Cr-C deposit was significantly increased from 597 Hv to 1636 Hv. The anneal-hardened Cr-C deposit is a suitable strengthening layer for fabricating electroplated diamond tools. The grinding performance of an electroplated diamond tool was strongly affected by the Ni-undercoating thickness. The highest maximum ground length of 2231 mm can be achieved by the electroplated diamond tool with a Ni-undercoating thickness of 90 μm. When the Cr-C strengthening deposit wore out, extruded diamond particles on the tool surface could be easily embedded into the Ni-undercoating, leading to fatigue fracture of the AISI 440C substrate.

Research Highlights

1. Electroplated diamond tools with 150-μm-sized diamond particles were fabricated.

2. A three-step electroplating processes was used to make electroplated diamond tools.

3. A Ni-undercoating thickness of 90 μm was suitable for making diamond tool.

4. Annealed Cr-C deposit is appropriate for strengthening diamond particles on the tool.

5. Fatigue fracture took place after extruded diamond particles were fully embedded.

1. Introduction

Owing to having extremely high hardness, synthetic diamond particles are widely used as abrasives and grinding particles for cutting and grinding hard-to-cut materials [1, 2], such as SiC and Al_2O_3 with high hardness and brittleness. To make grinding tools with diamond particles, composite electroplating is widely adopted because of its dimensional precision and economical production at a low temperature [3,4]. Thus, developing an appropriate electroplated diamond tool with high grinding performance is a promising pursue.

To fabricate electroplated diamond tools, composite electroplating is commonly used, where diamond particles in a size of few tens of micrometers are added in a metal-based plating bath [3,4]. A diamond-contained composite deposit can be achieved through reduction of metal ions with diamond particles

nearby the cathode or the tool substrate. The diamond density on the tool surface depends on the diamond concentration in the plating bath, electroplating current density, and diamond-particle size [5–7]. However, to achieve a composite deposit with diamond particles larger than 100 μm, composite electroplating is no longer viable because the stirred-up large diamond particles are unable to suspend in the plating bath solutions.

Many researchers [8] have proved that the grinding performance of an electroplated diamond tool depends strongly on the size of diamond particles on the tool surface. The larger diamond particles, the higher grinding performance of the tool [9,10]. Therefore, to grind a workpiece effectively, fabricating electroplated diamond tools with large diamond particles is essential. Based on our previous study [11], a three-step electroplating process, which include Ni-undercoating, Ni-diamond co-electrodeposition and strengthening electroplating, is suitable for making electroplating diamond tools with large diamond particles. In this study, diamond particles of an average size of 150 μm were utilized to fabricate electroplated diamond tools through the three-step electroplating process. Grinding performances of prepared tools were evaluated. Meanwhile, fractographic study of failed tools was conducted.

2. Experimental Procedure

As-purchased martensitic stainless-steel (AISI 440C) rods with a diameter of 3 mm were used as substrates for making electroplated diamond tools. Synthetic diamond particles with an average size of 150 μm were adopted for the process. Detail dimensions of prepared electroplated diamond tools are shown in Fig. 1, in which a tip length of 10 mm was electroplated with a single-layered of diamond particles. As shown in Fig. 2, the three electroplating processes, namely Ni-undercoating, Ni-diamond co-electrodeposition and Cr-C strengthening electroplating, were conducted to achieve a composite deposit with high diamond density [11].

To measure hardness values of as-plated and 500^{o}C-annealed Ni and Cr-C deposits. Ni and Cr-C deposits with a thickness of about 220 μm were prepared on the AISI 440C rod. The Ni deposit was electroplated in the Ni-Watt plating bath with a current density of 15 A/dm^2 at 50^{o}C for about 40 min. The Cr-C deposit was prepared at 30^{o}C with a current density of 30 A/dm^2 for about 180 min in the trivalent Cr plating bath [12,13]. Chemical compositions of the Ni-Watt plating bath are listed in Table 1. During Ni and Cr-C electroplating, the AISI 440C rod rotating at 100 rpm and a Pt-coated Ti mesh were set as working and counter electrodes, respectively. The hardness and standard deviation values of the prepared AISI 440C rod, Ni and Cr-C deposits were measured ten times with a load of 50 g by a micro-hardness tester (Matsuzawa Company, Model MXT-α7e).

Tools for grinding tests were first electroplated a layer of Ni-undercoating of varying thickness from 30 to 150 μm. Ni-diamond co-electrodeposition was then conducted through immersing the Ni-coated AISI 440C rod in an unwoven bag fully filled with diamond particles in the Ni-Watt plating bath. The Ni-diamond deposit was electroplated with a current density of 1.2 A/dm^2 for 90 min. A Ni deposit was further electroplated with a plating current density of 10 A/dm^2 in the Ni-Watt plating bath to effectively

increase Ni deposit thickness and to firmly fix extruded diamonds onto the AISI 440C rod. Finally, a Cr-C deposit was electroplated to fill vacancies between extruded diamond particles in a trivalent Cr plating bath. Electroplated diamond tools with diamond-coverage percentage of about 80% was obtained upon completion.

After completing the three-step electroplating process, electroplated diamond tools were annealed at 500^{o}C for 30 min and then cooled in the furnace to increase the hardness of Cr-C deposit and reduce the residual stress in the composite deposit. It was observed that an outward wash around the end side of tool was formed due to high charge concentration during electroplating. To grind a rectangular slot section, the outward wash was trimmed with electrical discharge machining (EDM) by using a Cu electrode with a diameter of 8 mm. During trimming, the end side of tool with an outward wash was set perpendicular to the middle of Cu-electrode surface. A current of 1.4 A was discharged with dielectric fluid flushing until the extruded wash was fully removed.

The grinding performances of prepared electroplated diamond tools were evaluated through linear slot-grinding of Al_2O_3 plates with a hardness of 1600 Hv. The slot grinding was performed by operating the milling machine (Ding Zhao Company, DZ-JW3040) at 15,000 rpm with a grinding depth and feed rate of 2 mm and 2 mm/min, respectively. During grinding, an amount of oil-contained coolant, which is suitable for grinding with electroplated diamond tools [14], was flushed directly at the grinding site. The maximum ground length as the grinding performance was recorded by averaging three diamond tools prepared under the same fabricating parameters.

For the fractographic study, cross sections of electroplated diamond tools were investigated after grinding to failure with an optical microscope (OM, Olympus BH2UMA) and a scanning electron microscope (SEM, HITACHI S-3000 N) equipped with energy-dispersive x-ray spectroscopy (EDS, Oxford INCA Energy 350).

3. Results And Discussion

3.1 Hardness test

Figure 3 shows hardness and standard deviation values of prepared AISI 440C substrate, Ni and Cr-C deposits. The hardness values of as-purchased AISI 440C remain relatively identical after annealing at 500^{o}C for 30 min. This implies that as-purchased AISI 440C rods had been quenched and tempered at a relatively high temperature to obtain a martensitic structure with a high toughness. The Ni deposit became softer after annealing at 500^{o}C. On the other hand, the hardness of as-plated Cr-C deposit increased from 597 Hv to 1636 Hv after annealing at 500^{o}C. According to our previous study [12,15], the anneal-hardening mechanism of Cr-C deposit could be attributed to the presence of diamond-like membranes. That is, prepared electroplated diamond tools could be firmly enclosed within the anneal-hardened Cr-C deposit. At the same time, the soft Ni-undercoating with an annealed hardness of 147 Hv could act as a buffer layer to absorb grinding impact between extruded diamond particles and the Al_2O_3

plate. It can be expected that the extruded diamond particles will gradually be compressed into the Ni-undercoating and prevent delamination, resulting an increased ground length.

3.2 Preparation of electroplated diamond tool

As shown in Fig. 2, the diamond-contained composite deposits of electroplated diamond tools were prepared through a three-step electroplating processes. In this study, the effect of Ni-undercoating thickness varying from 30 to 150 μm on the grinding performances of prepare electroplated diamond tools was investigated. After Ni-undercoating, Ni-diamond co-electrodeposition was conducted on the Ni-coated AISI 440C rod. As shown in Fig. 4(a), a high diamond density layer could be plated onto the AISI 440C rod surface after Ni-diamond co-electrodeposition. The diamond particles were fixed onto the Ni deposit with a thickness of about 30 μm. Upon strengthening with Cr-C electroplating at a plating current density of 10 A/dm^2, it was found that some extruded diamond particles were lost in the trivalent Cr plating bath. This is likely due to the evolution of hydrogen bubbles between extruded diamond particles during Cr-C electroplating, leading to dislodgement of some diamond particles from the tool surface. Thus, Ni electroplating with a thickness of 40 μm was further performed prior to Cr-C strengthening electroplating, as shown in Fig. 4(b). After increasing the Ni-deposit thickness to about 70 μm, a Cr-C deposit with a thickness of about 60 μm was successfully electroplated to strengthen diamond particles in the composite deposit, as shown in Fig. 4(c). The extruded diamond particles with an average height of about 20 μm from the tool surface allow for material cutting and removing Al_2O_3 powder-chips during slot grinding.

As shown in Fig. 4(c), the Cr-C strengthening deposit with a typical nodular surface can be seen on the tool surface after electroplating and annealing. Based on our previous study [11,12], some through-deposit cracks could be easily developed in the Cr-C deposit after annealing at temperature above 200^oC. However, surface cracks were not observed from the Cr-C deposit on the prepared tools after annealing at 500^oC for 30 min. This is because, according to our previous study [15], surface cracks can be significantly reduced through Cr-C-inert particles composite electroplating. Therefore, it can be expected that the crack-free Cr-C deposit provides sufficient strength to reinforce diamond particles on the tool surface.

As shown in Fig. 5(a), an obvious outward wash can be seen around the end of AISI 440C rod, owing to the charge concentration at the end corner during electroplating. To trim the outward wash, an electrical discharge machining (EDM) was adopted. Figure 5(b) shows the end side of tool trimmed with EDM. Figures 5(c) and (d) show cross sections of ground slots in Al_2O_3 plates. A rectangular slot was ground with the tool after EDM trimming; on the other hand, a bottom-enlarged slot was seen after grinding with untrimmed tool. To avoid the effect of outward wash around the end of the tool on the grinding performance, trimmed tools were used for the grinding tests in this study.

3.3 Grinding test

Figure 6 shows maximum ground lengths of prepared electroplated diamond tools with different Ni-undercoating thickness varying from 30 to 150 μm. The results indicate that the grinding performance of an electroplated diamond tool depends strongly on the Ni-undercoating thickness. A relatively short ground length of 357 mm was detected from the electroplated diamond tool with Ni-undercoating thickness of 30 μm. By further increasing the Ni-undercoating thickness to 60 μm and above, the maximum ground lengths of longer than 1450 mm can be achieved, which is more than four times than using 30 μm Ni-undercoating, as shown in Fig. 6. Overall, these ground lengths are much longer than those with electroplated diamond tools with multilayered 50-μm-sized diamond particles prepared in our previous works [4,11]. That is, with larger diamond particles, a higher grinding performance of tool was recognized. Due to anneal-softening, the annealed Ni-undercoating could be used as a buffer layer to absorb the grinding impact and force during grinding. The extruded diamond particles on the tool surface will be impacted and gradually compressed with increasing ground length. Therefore, it is crucial to have an optimal undercoating thickness with respect to the size of diamond particles. As the results indicated, the 30-μm-thick Ni-undercoating in the electroplated diamond tool cannot sufficiently bear the grinding impact, leading to low grinding performance. Thus, a thickness of 30 μm is not suitable for the proposed tool fabrication with 150-μm-sized diamond particles. On the other hand, with the highest maximum ground length of 2231 mm, the Ni-undercoating thickness of 90 μm is desirable.

3.4 Fractographic study

To clarify the effect of Ni-undercoating thickness on grinding performances, surface morphologies and cross sections of electroplated diamond tools with Ni-undercoating thickness of 30, 90 and 120 μm were examined after grinding to failure. Cr-K_α-line scanning with EDS along the cross sections of failed tools are shown in Figs. 7–9. Figures 7(a) and (b) depict a Cr-C deposit with a nodular surface on the electroplated diamond tool prepared with a 30-μm-thick Ni-undercoating after grinding test. As shown in Fig. 7(a), some wide cracks were observed from the tool surface. Moreover, obvious delamination between the diamond-contained composite deposit and the Ni-undercoating was seen from the cross section of the failed tool shown in Fig. 7(b). The Cr-C strengthening deposit can be realized from the result of Cr-K_α-line scanning with EDS from site A to site B shown in Fig. 7(c), from which the Cr-K_α radiation along a deposit thickness of about 50 μm was detected. This means that most of the Cr-C deposit did not wear out upon tool failure at the ground length of 357 mm.

As shown in Figs. 8(a) and (b), cracking of the Cr-C strengthening deposit was not found from the tool with Ni-undercoating thickness of 90 μm, which was evidenced to be an optimal thickness for obtaining the highest tool performance. Moreover, delamination between diamond-contained composite deposit and the Ni-undercoating was not observed, as shown in Fig. 8(b). The surface morphology of the tool was flattened, and extruded diamond particles were almost compressed into the Ni-undercoating. From the result of Cr-K_α-line scanning with EDS from site A to site B shown in Fig. 8(c), Cr-K_α radiation was not detected in the range of the Cr-C strengthening deposit. This indicates Cr-C deposit was almost worn out after grinding to failure. It can be reasonably assumed that the extruded diamond particles on the tool

surface were compressed into the Ni-undercoating quickly when the anneal-hardened Cr-C deposit layer was depleted.

As shown in Fig. 9(a), a network of thin cracks and diamond particles leveled together with the Ni-undercoating were seen from the tool surface with a Ni-undercoating thickness of 120 μm. Similar to the tool with 90-μm-thick Ni-undercoating, interfacial delamination and thin cracks were not seen from the cross section of the tool shown in Fig. 9(b). From the result of Cr-K_{α}-line scanning with EDS from site A to site B shown in Fig. 9(c), Cr-K_{α} radiation was not found on the surface of the tool. This means that the anneal-hardened Cr-C deposit wore out after grinding to failure, leading to embedding of diamond particles into the Ni-undercoating. The extruded diamond particles on the tool with a relatively thick Ni-undercoating thickness of 120 μm could be embedded after Cr-C deposit was fully worn out. A thin net of surface cracks was developed when grinding proceeded.

Figure 10a) and b) depict failed tools with 30- and 60-μm-thick Ni-undercoating from grinding tests, respectively. It can been seen from Fig. 10a) that the diamond-contained composite deposit peeled off from the tool surface. This fully agrees with the observation on the surface and the cross section of the failed tool shown in Fig. 7(a) and (b), in which interfacial delamination and cracking were seen. Once the diamond-contained composite deposit peeled off from the tool surface, the AISI 440C substrate was apparently worn because of different hardness between the Al_2O_3 plate and the AISI 440C rod. Because Al_2O_3 plates were produced through powder metallurgy, the removal of Al_2O_3-powder chips by the extruded diamond particles are essential. Owing to difficulty in removing Al_2O_3-powder chips, a high grinding force is experienced when the diamond particles are fully embedded into the Ni-undercoating. Because the tool rod was bent during grinding with a grinding feed of 2 mm/min and a rotational speed of 15,000 rpm, the rod was subjecting a cyclic stress. The stress amplitude increased greatly when the extruded diamond particles were fully embedded into the Ni-undercoating. As higher stress amplitude was applied, a shorter fatigue life was recognized. Fatigue failures of AISI 440C rod were found from the tools with Ni-undercoating thickness varying from 60 to 150 μm after extruded diamond particles were leveled with the Ni-undercoating. Figure 10(b) shows the fatigue fracture of failed AISI 440C rod from the tool with Ni-undercoating thickness of 90 μm. The fatigue fracture can be characterized by almost no plastic deformation and flat fracture morphology as shown in the figure.

4. Conclusion

Based on experimental results, some conclusions can be drawn as the following:

1. Electroplated diamond tools with single-layered diamond particles and high diamond density can be successfully prepared through the three-step electroplating process.

2. The grinding performance of an electroplated diamond tool depends strongly on the Ni-undercoating thickness. The Ni-undercoating with a thickness of 30 μm is insufficient to absorb grinding impact,

leading to cracking and peeling of diamond-contained composite deposit. The highest grinding performance can be achieved from the tool prepared with a Ni-undercoating thickness of 90 μm.

3. Extruded diamond particles could be easily embedded into the Ni-undercoating and losing their grinding abilities when the anneal-hardened Cr-C deposit fully wore out. This eventually resulted the fatigue failure of the tested tools.

Declarations

Funding: This work was supported by Chang Gung Medical Foundation in Taiwan [Grant numbers: CMRPD2L0091]. The grant was awarded to Dr. Ching An Huang.

Competing interest: The authors have no competing interests to declare that are relevant to the content of this article.

Availability of data and material: Not applicable.

Code availability: Not applicable.

Ethics approval: Not applicable.

Consent to participate: Not applicable.

Consent for publication: Not applicable.

References

[1] Gupta RK, Pratap B (2021) Diamond tools processing for marble and granite: Cutting & wear. In: Materials Today: Proceedings 46:2135-2140. https://doi.org/10.1016/j.matpr.2021.02.346

[2] Zhang H, Zhang J, Wang Z, et al (2016) A new frame saw machine by diamond segmented blade for cutting granite. Diam Relat Mater 69:40-48. ttps://doi.org/10.1016/j.diamond.2016.07.003

[3] Wang X, Chou CC, Lee JW, et al (2020) Preparation and investigation of diamond-incorporated copper coatings on a brass substrate by composite electrodeposition. Surf Coatings Technol 386:125508. https://doi.org/10.1016/j.surfcoat.2020.125508

[4] Huang CA, Yang SW, Shen CH, et al (2019) Fabrication and evaluation of electroplated Ni–diamond and Ni–B–diamond milling tools with a high density of diamond particles. Int J Adv Manuf Technol 104:2981-2989. https://doi.org/10.1007/s00170-019-04174-3

[5] Zhou H, Zhu L, Qian Z, et al (2014) Codeposition process of Ni-diamond. Rare Met Mater Eng. 43:2177-2181.

[6] Li S, Gao YF (2020) Effect of abrasive density on sawing performance of electroplated diamond wire. Manuf Technol Mech Tool 6:104-107.

[7] Lee EC, Moon IT (2002) Electrolytic codeposition of diamond particles with nickel and cobalt metals. Plat Surf Finish.

[8] Deja M, Zieliński D (2020) Wear of electroplated diamond tools in lap-grinding of Al_2O_3 ceramic materials. Wear. https://doi.org/10.1016/j.wear.2020.203461

[9] Shi Z, Malkin S (2006) Wear of electroplated CBN grinding wheels. J Manuf Sci Eng Trans ASME 128:110-118. https://doi.org/10.1115/1.2122987

[10] Wu Y, Luo J, Wang Y, et al (2019) Critical effect and enhanced thermal conductivity of Cu-diamond composites reinforced with various diamond prepared by composite electroplating. Ceram Int 45:13225-13234. https://doi.org/10.1016/j.ceramint.2019.04.008

[11] Huang CA, Shen CH, Yang SW, et al (2020) Fabrication and evaluation of electroplated diamond grinding rods strengthened with Cr-C deposit. Int J Adv Manuf Technol 110:2541-2550. https://doi.org/10.1007/s00170-020-05989-1

[12] Huang CA, Liu YW, Yu C, Yang CC (2011) Role of carbon in the chromium deposit electroplated from a trivalent chromium-based bath. Surf Coatings Technol 205:3461-3466. https://doi.org/10.1016/j.surfcoat.2010.12.010

[13] Huang CA, Yang SW, Liu YW, Lai PL (2019) Effect of Cu and Ni undercoatings on the electrochemical corrosion behaviour of Cr-C-coated steel samples in 0.1 M H_2SO_4 solution with 1 g/L NaCl. Coatings 9:531. https://doi.org/10.3390/coatings9090531

[14] Choudhary A, Paul S (2020) The wear mechanisms of diamond grits in grinding of alumina and yttria-stabilized zirconia under different cooling-lubrication schemes. Wear. https://doi.org/10.1016/j.wear.2020.203315

[15] Huang CA, Chen JY, Chuang CH, Mayer J (2017) Properties of Cr–C–Al2O3 Deposits Prepared on a Cu Substrate Using Cr3+-Based Plating Baths. Powder Metall Met Ceram 55:596-602. https://doi.org/10.1007/s11106-017-9844-1

Tables

Table 1
Chemical compositions of Ni-Watt electroplating bath used in this study.

Component	Concentration (g/L)
$NiSO_4$	300
NiCl	50
H_3BO_3	40
SDS	3
SDS: Sodium dodecyl sulfate	

Figures

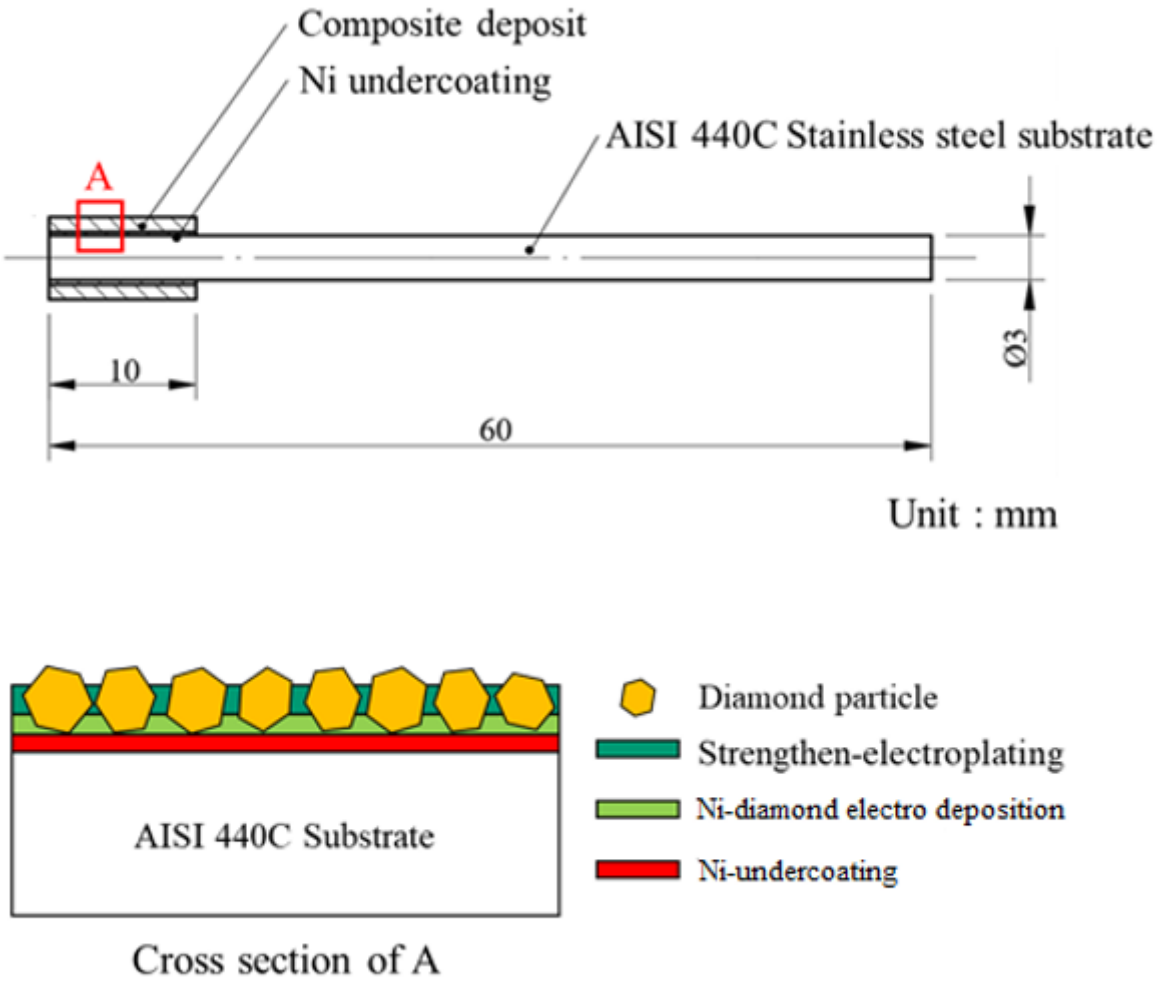

Figure 1

Dimensions of electroplated diamond tools with single-layered diamond particles prepared in this study.

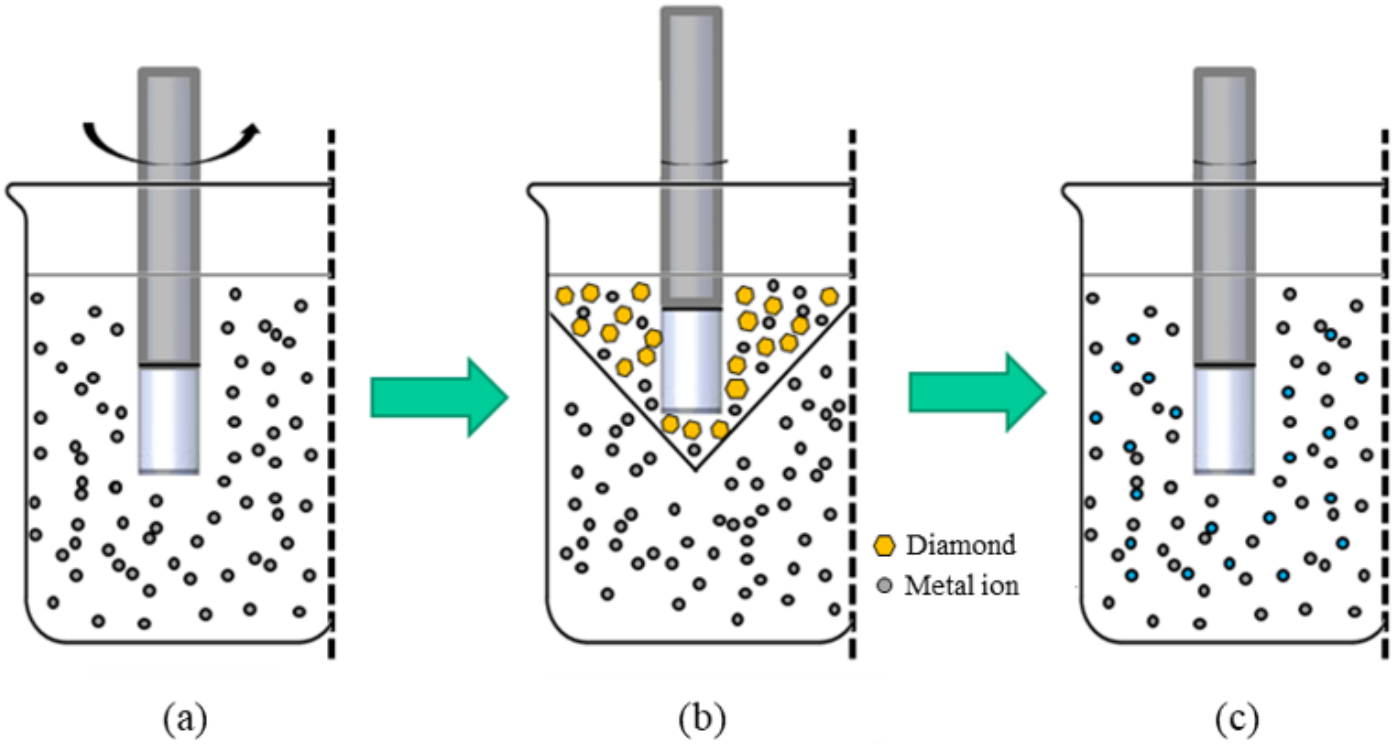

Figure 2

The three-step electroplating process: (a) Ni undercoating, (b) Ni-diamond co-electrodeposition, and (c) Cr-C strengthening electroplating.

Figure 3

Hardness variation of prepared tool materials: (a) as-purchased AISI 440C, (b) 500^{o}C-annealed AISI 440C, (c) as-plated Ni-undercoating, (d) 500^{o}C-annealed Ni-undercoating, (e) as-plated Cr-C deposit and (f) 500^{o}C-annealed Cr-C deposits.

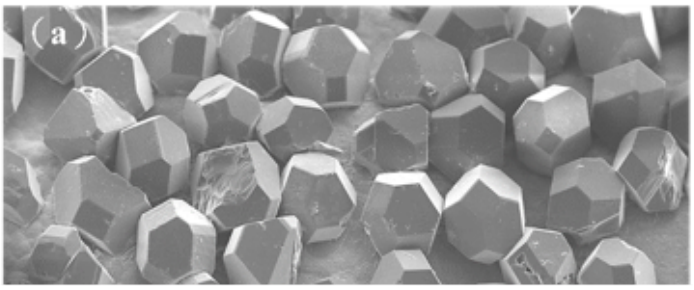

Figure 4

Surface morphologies of an electroplated diamond tool after (a) Ni-diamond co-electrodeposition, (b) Ni electroplating and (c) Cr-C strengthening electroplating.

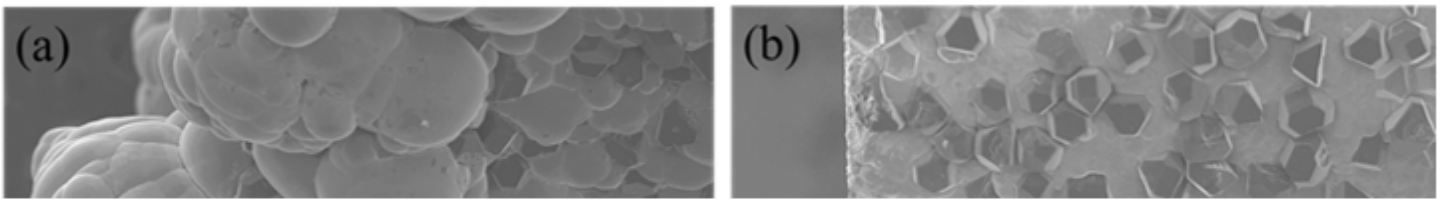

Figure 5

End sides of electroplated diamond tools (a) before, and (b) after trimming with EDM. Side views of ground slots in the Al_2O_3 plate with (c) untrimmed, and (d) trimmed electroplated diamond tools.

Figure 6

Maximum ground lengths of electroplated diamond tools strengthened with Cr-C deposits in relation to different Ni-undercoating thicknesses.

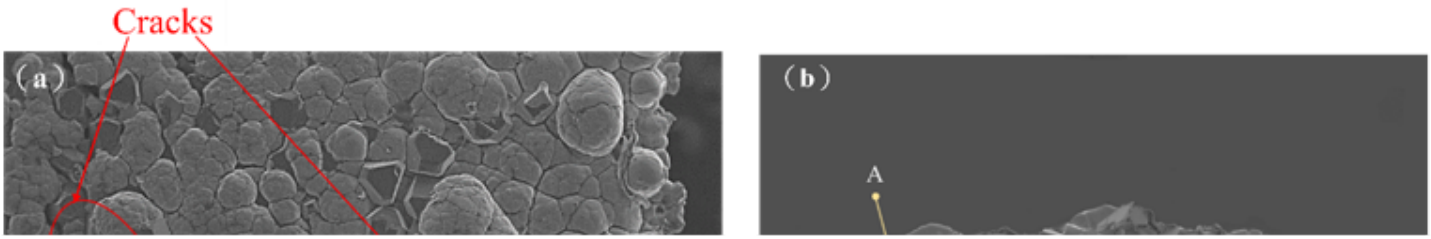

Figure 7

Electroplated diamond tool with Ni-undercoating thickness of 30 μm after grinding to failure, showing its (a) surface morphology and (b) cross section. (c) Cr-Kα-line scanning with EDS from A to B presented in (b).

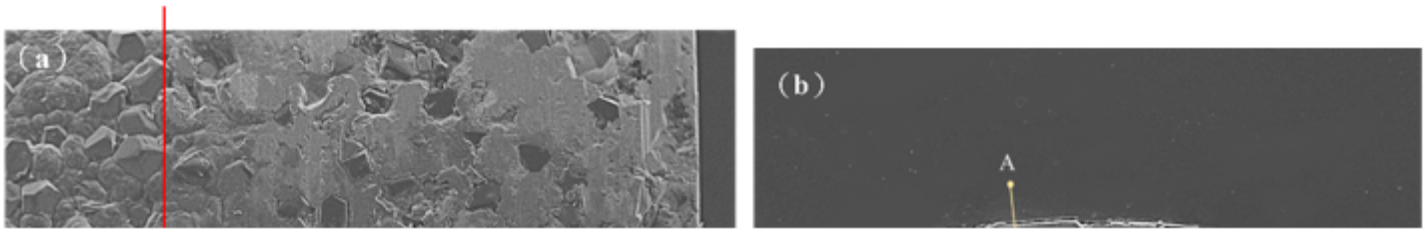

Figure 8

Electroplated diamond tool with Ni-undercoating thickness of 90 μm after grinding to failure, showing its (a) surface morphology and (b) cross section. (c) Cr-Kα-line scanning with EDS from A to B presented in (b).

Figure 9

Electroplated diamond tool with Ni-undercoating thickness of 120 μm after grinding to failure, showing its (a) surface morphology and (b) cross section. (c) Cr-Kα-line scanning with EDS from A to B presented in (b).

Figure 10

(a) Peeling of diamond-contained composite deposit with Ni-undercoating thicknesses of 30 μm, and (b) fatigue fracture of AISI 440C rod piece from the diamond tool with Ni-undercoating thicknesses of 90 μm after grinding to failure.